

Review

Recent Development of Photocatalytic Application Towards Wastewater Treatment

Preetam Datta, Subhasis Roy *

Department of Chemical Engineering, University of Calcutta, 92 A.P.C Road, Kolkata, India; E-Mail: preetamdatta95@gmail.com; subhasis1093@gmail.com; srchemengg@caluniv.ac.in* **Correspondence:** Subhasis Roy; E-Mails: subhasis1093@gmail.com; srchemengg@caluniv.ac.in**Academic Editor:** Youliang Cheng**Special Issue:** [Photocatalysis for Water and Wastewater Treatment](#)*Catalysis Research*
2023, volume 3, issue 3
doi:10.21926/cr.2303020**Received:** April 15, 2023**Accepted:** June 27, 2023**Published:** July 05, 2023

Abstract

With increasing population levels and rapidly growing industries worldwide, the purification of water contaminated with different impurities is one of the biggest challenges we face in recent times. Photocatalysis holds great potential as an efficient mineralization process to remove the foreign matter present in wastewater. Rapid advancement in innovative materials development has made photocatalysis the frontrunner among different water treatment methods. Our main priority lies in different strategic approaches to improve photocatalytic performance. This review discusses the recent breakthrough in implementing the photocatalytic mechanism for successful wastewater treatment. Challenges and future prospects in this technological field have also been discussed.

Keywords

Water pollution; photocatalysis; wastewater treatment; purification; contaminants



©2023 by the author. This is an open access article distributed under the conditions of the [Creative Commons by Attribution License](#), which permits unrestricted use, distribution, and reproduction in any medium or format, provided the original work is correctly cited.

1. Introduction

In recent times, water pollution has turned out to be a major problem mainly due to the rapid advancement in the industrial sector, creating adverse effects on marine life and the ecosystem. Such pollution also adds to an enhancement in water treatment costs owing to the recalcitrant nature of some pollutants, for instance, dyes, pharmaceuticals, surfactants, personal care products, and many others [1]. Organic dyes and their intermediates release carcinogenic, mutagenic or teratogenic components into the water bodies through different oxidation and hydrolysis reactions, harming aquatic life [2, 3]. Wastewaters containing recalcitrant components generally possess high chemical oxygen demand (COD), intense color, total dissolved solids (TDS) content, inconsistent pH, and low biodegradability. The performance of a solar photocatalysis reactor as a pretreatment for wastewater to control membrane fouling was observed recently [4]. An alteration to the natural water cycle might hamper energy and crop production, human health, and economic development, which might significantly hinder our sustainable development goals, as identified by the United Nations' World Water Development Report (2020). For this reason, research on modernized, environmentally sustainable, cost-effective, and productive methods for the redemption of wastewater have become necessary.

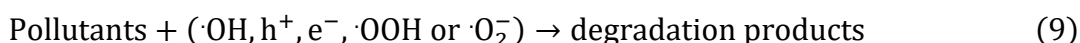
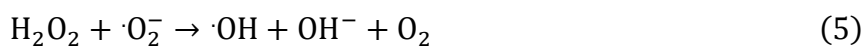
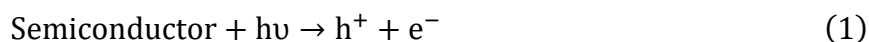
In order to develop an aquatic environment free from pollutants, it is inevitable to treat the water-laden toxic organic components. Several state-of-the-art technologies are available for application in wastewater purification, which includes electro dialysis [5], membrane filtration [6], precipitation [7], adsorption [8-11], electrochemical reduction [12], and electro deionization [13, 14]. However, such conventional processes are inefficient since they consume a large amount of energy apart from giving rise to sludge formation and generating secondary pollutants. Advanced oxidation processes (AOPs) have the potential to effectively decompose such harmful and toxic pollutants by generating strong oxidizing agents, such as hydroxyl radicals ($\cdot\text{OH}$), which have been proven to be efficient enough in completely mineralizing toxic organic pollutants. However, many AOPs necessitate supplementary chemicals as oxidants and extra energies, intensifying the energy crunch. In the current era, semiconductor photocatalysis, with non-conventional solar energy, as its driving force, is one such AOP process, which has been extended in wastewater treatment mainly due to its potential to remove various contaminants from water with the improvement of the drawbacks set by other advanced oxidation processes (AOPs) for instance highly-priced, imperfect decomposition and many others [3, 4]. Photocatalysis was introduced later to treat contaminated water containing dyes, pharmaceuticals, and other harmful substances by degrading complex compounds in wastewater to less harmful substances like water, carbon dioxide, or other small molecules under solar irradiation.

In this review, we will focus on the recent advancement in wastewater treatment using the photocatalysis technique and accentuate the design and development of those materials. By understanding the current research advancement, we are hopeful enough to discuss the recent modifications in photocatalyst development and their reaction mechanisms in the effective removal of contaminants from water, along with newer ideas and prospects towards the future development of complex structured photocatalysts and their composite systems in water waste treatment.

2. Basic Principles of Semiconductor Photocatalysis

The major objective of the photocatalytic mechanism is to stimulate or accelerate redox reactions when a light source illuminates the semiconductor. During photocatalysis, when a semiconductor is excited by photons with energy equivalent to (or higher than) the band gap energy (E_g), an electron (e^-) of the valence band (VB) is upgraded to the conduction band (CB), resulting in the formation of a hole (h^+) in the VB. Therefore a pair of photogenerated e^- and h^+ is generated. This pair would migrate to the surface of the semiconductor. However, there is a tendency for these excited electrons and holes might recombine, resulting in the generation of phonons or heat, thereby causing a reduction in the number of electrons and holes. The resultant electrons act as a reductant to directly bring down some hefty metal ions. The reaction between the splitter holes having a hydroxyl ion (OH^-) or a water molecule leads to hydroxyl radicals ($\cdot OH$).

Additionally, In Figure 1 shows the schematic diagram of photodegradation of an organic pollutant under sunlight via tricobalt tetroxide nanoparticles (Co_3O_4 NPs) [12]. This photo-separated electrons may perform with dissolved oxygen of water to liberate superoxide radicals ($\cdot O_2^-$), which give rise to $\cdot OH$ upon additional reaction. At first, the impurities in the water get adsorbed on the external part of the photocatalyst, enhancing the movement of charge and intensifying its redox ability. This phenomenon leads to a string of chemical reactions in connection with the active variants brought about by the photocatalyst, which gives the final degradation products [15]. The redox reactions are listed as follows (Equations (1)–(9)):



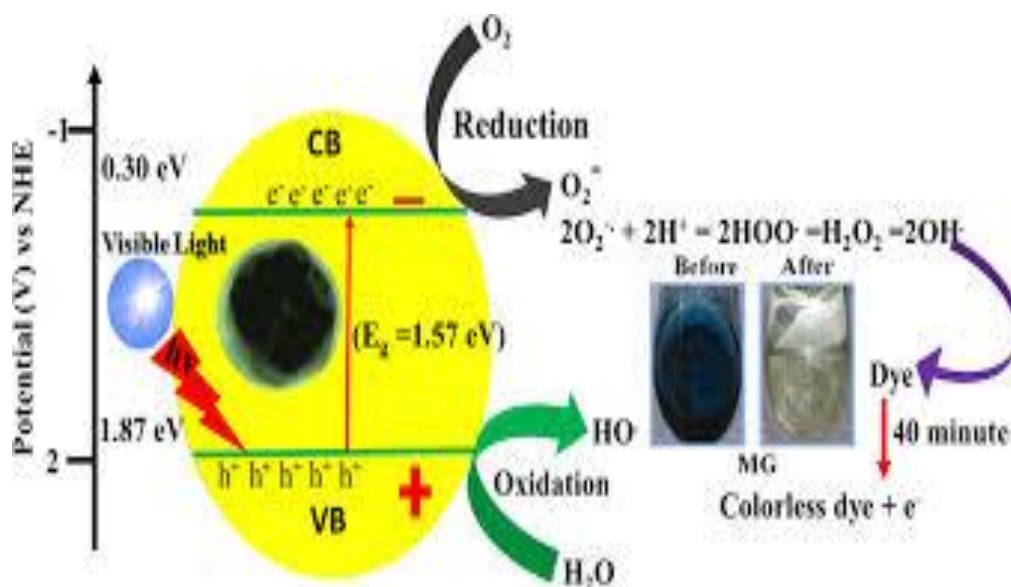


Figure 1 Schematic diagram showing photodegradation of an organic pollutant under sunlight via tricobalt tetroxide nanoparticles (Co_3O_4 NPs) [12]. (Reproduced with permission).

In order to reduce the rate of recombination of the photogenerated charge carriers during photocatalysis, there is a necessity for the creation of a suitable heterojunction. A heterojunction is a boundary space that normally appears amongst two semiconductors with unlike band structures, resulting in band sequencing. In a heterojunction photocatalyst, two semiconductors work in conjunction in a synchronized fashion, which curtails the effect of recombination. Here, the photogenerated charge carriers proceed through the system due to the proper interactivity of semiconductor-based materials, thereby enhancing the separation efficiency. Apart from this, heterojunction photocatalysts have several other benefits; for instance, heterojunctions can improve the light-harvesting capacity to a much higher wavelength. Since approximately 50% of the solar spectrum consists of visible light, integrating a semiconductor-incorporated photocatalyst helped to intensify the absorption of visible light to a greater wavelength region. Additionally, combining one semiconductor with another might help achieve increased photocatalytic activity. Consequently, the heterojunctions improved the availability of more reactive substances which helped to increase the degradation efficiency [16].

Depending upon various band and electronic arrangements, the heterojunctions can be grouped into six types, namely, traditional (for example, type-I (straddling gap), type-II (staggered gap), and type-III (broken gap) heterojunctions), p-n, Z-scheme, S scheme, and Schottky heterojunctions. Different heterojunction structures result in varying photocatalysis mechanisms to inhibit the recombination of photogenerated charge carriers [16].

2.1 Type-I Heterojunction

In Type-I heterojunction, the CB and VB of the first semiconductor are greater and lesser than the corresponding bands of the second one. Under visible light irradiation, the photoexcited charge carriers move to the CB and VB bands of the second semiconductor. Since most of the photogenerated electrons and holes accumulate within the same semiconductor, it is impossible to

efficiently set apart the electron-hole pairs, enhancing the recombination process. Additionally, the photocatalytic reactions in type-I heterojunction have lower oxidation and reduction potentials, leading to reduced photocatalytic activity under visible light irradiation [17, 18]. For instance, as a type-I photocatalyst, the magnet silica-coated $\text{Ag}_2\text{WO}_4/\text{Ag}_2\text{S}$ nanocomposites (FOSOAWAS) efficiently removed Congo red dye from wastewater within 140 min of visible-light irradiation. Here, the direct contact between Ag_2WO_4 and Ag_2S in the FOSOAWAS composite helped to develop Type I heterojunction after absorption of visible light, which resulted in enhanced electron-hole separation and inhibited their recombination process [19].

2.2 Type-II Heterojunction

In Type-I heterojunction, the CB and VB of the first semiconductor are greater than the corresponding bands of the second one. Therefore, under visible light irradiation, the photoexcited electrons move to the second semiconductor, while the photoexcited holes move to the first semiconductor, leading to an effective electron-hole separation process; thereby, the charge recombination tendency is lowered [20]. Alike type-I heterojunction photocatalyst, in type-II heterojunction photocatalyst, since the reduction and the oxidation reactions amongst the two semiconductors happen with lessened reduction and oxidation potential, respectively, the redox ability of this heterojunction is diminished, resulting in reduced photocatalytic activity [21]. This type of heterojunction is the most successful heterojunction structure, useful to improve photocatalytic performance since it possesses an appropriate structure for effective dissociation of electron-hole pairs [17, 18]. For instance, a type-II $\text{CuS}/\text{BiFeO}_3$ heterojunction showed more than 90% alachlor pesticide decomposition only within 60 mins. The band positions of the two components, CuS and BiFeO_3 were aligned favorably in order to get a cyclic movement of photogenerated electrons and holes, resulting in a type-II heterojunction, which was mainly responsible for the effective photodegradation mechanism and the inhibition of recombination by the ternary composite structure [22].

2.3 Type-III Heterojunction

Here, the structure is quite close to the type-II heterojunction photocatalyst. Only the staggered gap is large enough to inhibit the overlapping of the bandgaps. For this reason, the drift and dissociation of the photogenerated electron-hole pairs between the two semiconductors cannot occur in the case of the type-III heterojunction, making it inappropriate for effectively separating the charge carriers [23, 24].

2.4 p-n Heterojunction

Even though the type-II heterojunction photocatalyst can effectively inhibit the recombination of photoexcited charge carriers in space, the attained improvement in the separation of charge carriers over the type-II heterojunction is not adequate to get better high-speed recombination process of the photoexcited electrons and holes on the semiconductor. In order to overcome this defect, the movement of electron-hole pairs through the heterojunction can be improved by adding a supplementary electric field, which leads to the formation of a p-n heterojunction photocatalyst. The combination of a p-type semiconductor and an n-type semiconductor generally obtains a p-n

heterojunction photocatalyst. In case of a n-type semiconductor, the Fermi level is located close to the CB of the semiconductor. In contrast, in a p-type semiconductor, the Fermi level is located close to the VB of the semiconductor. Before the irradiation of visible light, the photoexcited electrons across the n-type semiconductor close to the p–n junction tend to disperse towards the p-type semiconductor, leaving behind positively charged strains. On the other hand, the photoexcited holes across the p-type semiconductor close to the p–n junction tend to disperse towards the n-type semiconductor, leaving behind negatively charged strains. The diffusion between the photogenerated electron–hole pairs will continue until the process's Fermi level equilibrium is accomplished [17, 18]. This leads to forming an internal electric field nearby the p-n junction. Upon visible light irradiation on the p-type and n-type semiconductors, pairs of photoexcited electrons and holes are generated. These pairs of electrons and holes in the p-type and n-type semiconductors travel along to the CB of the n-type semiconductor and the VB of the p-type semiconductor, respectively, due to the effect of the internal electric field, leading to contiguous separation of the electron–hole pairs. In the p-n heterojunction photocatalyst, the CB and the VB of the p-type semiconductor are generally based upon a higher position than those of the n-type semiconductor. Due to this factor, the effectivity of the electron–hole dissociation in p–n heterojunction photocatalysts is faster than that of the type-II heterojunction photocatalysts, which is ascribed to the coordination between the internal electric field and the band orientation [20].

2.5 S Scheme Heterojunction

The S-scheme or step scheme heterojunction system was first observed by Yu et al. [25] in 2018, between two n-type semiconductors, having a staggered band alignment, quite similar to the type-II heterojunction system, except for one change, which is the dissimilar pathway of transport of charged species [26]. In this heterojunction, one semiconductor possesses a lower work function (WF) with a higher Fermi level, while another possesses a higher WF with a lower Fermi level. When the two semiconductors come close to each other, there is an interfacial flow of electrons from the higher Fermi level to the lower Fermi level. Due to this, the interfaces among the two semiconductors are positively and negatively charged, respectively, leading to an internal electric field [27]. This phenomenon gives rise to the bending of energy bandgaps of the two semiconductors. In response to the visible light, the photoexcited electrons from the CB of the semiconductor having lower Fermi level travel to the VB of the semiconductor having a higher Fermi level within the internal electron field, which leads to the effective implementation of photogenerated electrons and holes over CB and VB of both the semiconductors respectively [17, 28]. For instance, Jabbar et al. [29] developed a novel dual S scheme $g\text{-C}_3\text{N}_4/\text{Ag}_2\text{WO}_4/\text{Bi}_2\text{S}_3$ heterojunction nanostructure to completely decompose Congo red dye under visible light irradiation. In such a scheme, the stacked electrons in the CB of $g\text{-C}_3\text{N}_4$ migrated to the VB of Ag_2WO_4 and Bi_2S_3 semiconductors and recombined with their stacked holes. On the other hand, a superior negative potential (-1.148 eV) and a suitable positive potential (3.02 eV) were developed on the CB of $g\text{-C}_3\text{N}_4$ and the VB of Ag_2WO_4 , respectively. Therefore, the dissolved oxygen and H_2O or/and OH^- were occupied by free electrons and holes, respectively, in the redox reactions, thereby releasing $\cdot\text{OH}$, $\cdot\text{O}_2^-$ along with H_2O_2 oxidants, which were successful in decomposing the Congo red dye to simpler products.

2.6 Schottky Heterojunction

A Schottky heterojunction is generally formed by the junction of a semiconductor with a metal, leading to an effective space-charge zone [30, 31]. The electrons proceed faster from one material to another at the junction of the two species. Therefore, the Fermi energy levels' alignment takes place, resulting in a reduced electron-hole recombination rate, which leads to enhanced photocatalytic activity performance [31]. For instance, Wu et al. [32] discovered a $g\text{-C}_3\text{N}_4/1\text{T-MoS}_2$ Schottky heterojunction photocatalyst, which positively affected the successful treatment of nuclear plant wastewater. Here, the semiconductor/metal heterojunction, also known as the Schottky barrier, resulted in the enhanced separation of photogenerated electron and hole, and the electrons migrated from the semiconductor to the conductor as a result of the alignment of Fermi energy levels, thereby creating a restriction in recombination of photogenerated charge carriers. A Schematic diagram showing removal of organic pollutants by the $g\text{-C}_3\text{N}_4/1\text{T-MoS}_2$ heterojunction under visible light irradiation shows in Figure 2 [32].

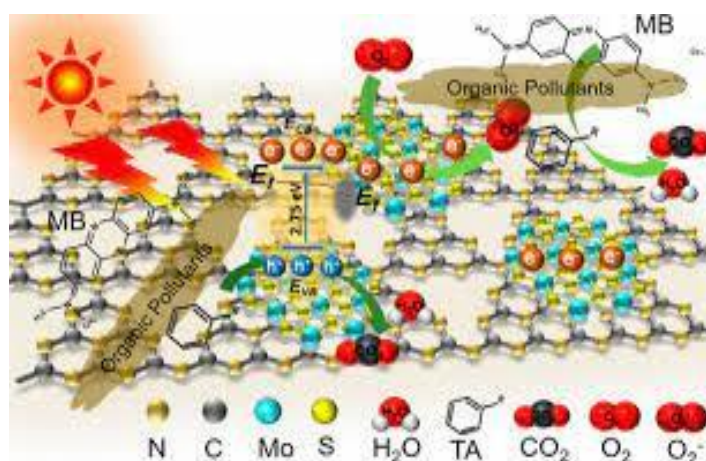


Figure 2 Schematic diagram showing removal of organic pollutants by the $g\text{-C}_3\text{N}_4/1\text{T-MoS}_2$ heterojunction under visible light irradiation [32] (Reproduced with permission).

2.7 Z Scheme Heterojunction

A Z-scheme heterojunction composite comprises a band structure similar to the Type-II heterojunction. However, the charge transfer mechanism differs from the Type-II heterojunction [20]. The conventional drawbacks of the Type-II heterojunction photocatalyst include a depletion in redox potential with energy dissipation, resulting in adversity in the migration of electrons from the CB and holes from VB to the respective CB and VB, respectively [18]. Such drawbacks can be overcome with the development of a Z-scheme photocatalyst. In the Z-scheme photocatalysts, the oxidation reaction takes place on the semiconductor surface, with greater oxidation ability and reduction with greater redox potential. Due to this, the photogenerated charge transfer in the Z-scheme heterojunction photocatalyst occurs due to electrostatic attraction between photogenerated electrons and holes, which is much simpler than the Type-II heterojunction [33]. For instance, a 2D/2D Z-scheme heterostructure photocatalyst of BiOBr/TzDa covalent organic framework (COF) composite. Here, it was observed that RhB was oxidized mainly by h^+ and $\cdot\text{O}_2^-$, and photo-generated electrons enhanced in the reduction of Cr(VI) to Cr(III). The redox reactions of $\text{RhB}-h^+$ and $\text{Cr(VI)}-e^-$ were simultaneously carried out in the system of $\text{BTDC}/\text{RhB}/\text{Cr(VI)}$, which

created an enhancement in the spatial separation of electrons and holes, thus endowing BTDC with higher potential in the decomposition of Cr(VI) and RhB at the same time [34].

2.8 Photocatalyst Materials for Wastewater Treatment

Recent reported photocatalyst materials for wastewater treatment depicted in Table 1.

Table 1 Summary of some of the photocatalyst materials for wastewater treatment.

Sl No.	Semiconductor or materials	Advantages	Drawbacks	References
1.	g-C ₃ N ₄	<ul style="list-style-type: none"> The small and tunable band gap (2.7 eV) High surface area suitable for efficient light absorption Low-cost, non-toxic, and chemically as well as thermally stable 	<ul style="list-style-type: none"> Fast recombination of photogenerated electron-hole pairs 	[35, 36]
2.	ZnO	<ul style="list-style-type: none"> High surface reactive and chemically stable Low-cost, high electrochemical coupling coefficient, and high photostability 	<ul style="list-style-type: none"> High rate of recombination of photoexcited charge carriers Photocatalytic activity limited to UV region only due to the wide energy band gap (3.37 eV) Limited visible-light responsive region 	[37-40]
3.	BiOBr	<ul style="list-style-type: none"> The small and tunable band gap (2.8 eV) Intrinsic layered crystal structure leading to efficient photogenerated charge separation 	<ul style="list-style-type: none"> Low adsorption capacity 	[41-45]
4.	ZnFe ₂ O ₄	<ul style="list-style-type: none"> The narrow band gap (1.9 eV) Spinel crystallographic structure showing excellent photochemical stability 	<ul style="list-style-type: none"> High rate of photocorrosion as well as agglomeration High rate of recombination of 	[46-48]

		<ul style="list-style-type: none"> • Can be efficiently recycled in water treatment and purification systems 	photogenerated charge carriers	
5.	CuO	<ul style="list-style-type: none"> • Narrow bandgap of 1.4 eV enhances high visible-light absorption capacity • High rate of recombination of photogenerated charge carriers • High rate of recombination of photogenerated charge carriers • High photocurrent density of 35 mA/cm² at 0 V vs. RHE 	<ul style="list-style-type: none"> • Fast electron-hole recombination rate • Lack of generation of reactive oxygen species (ROS) 	[39, 46, 49]
6.	TiO ₂	<ul style="list-style-type: none"> • Low-cost, eco-friendly, non-toxic, high chemical stability • Low minority charge-carrier diffusion length 	<ul style="list-style-type: none"> • Only UV in the solar spectrum (about 3–5%) can be utilized to carry out photocatalytic reactions due to the large band gap of TiO₂ (3.2 eV) • Lower separation efficiency of electron-hole pairs 	[50-52]

3. Removal of Organic Compounds

Various types of organic pollutants in wastewater include pesticides, dyes, surfactants, phenolic components, pharmaceuticals, chloro-organics, plasticizers, organohalides, and many others [53-55]. These materials are very toxic and may pose severe environmental threats to nature and human health if they are decomposed following traditional techniques. Therefore, the photocatalysis mechanism decomposes the organic contaminants in wastewater into less harmful organic products such as H₂O, CO₂, NO₃⁻, PO₄⁻³, and other halide ions [56]. Various types of semiconducting materials, for instance, TiO₂ [57], ZnO[58], Bi₂MoO₆[59], and Cu₂O [60] have been investigated to degrade excellently an expansive area of organic contaminants into easily degradable or harmless products.

3.1 Dyes

Dyestuff present in wastewater is lethal and sometimes carcinogenic to humans, aquatic plants, animals, and other microorganisms [61]. Heterogeneous photocatalysis appeared to be very effective since it can completely degrade dye effluents to less harmful substances such as H_2O , CO_2 , etc., making it a very useful process for safely releasing textile wastewater into water bodies [62]. Lafta et al. [36] incorporated phosphotungstic acid (PTA) upon metal-free graphitic carbon nitride ($\text{g-C}_3\text{N}_4$), which efficiently degraded more than 90% methyl violet dye (MV), present in wastewater at a pH value of 6.8, within a very short time. Such enhanced performance was attributed to PTA's high electron-hole separation efficiency. Yan et al. [63] developed a novel $\text{BiVO}_4/\text{Ag}_3\text{VO}_4$ heterojunction photocatalyst for decomposing rhodamine B (RhB) pollutants in wastewater. The study revealed 95.9% degradation rate of RhB, much higher than the respective BiVO_4 and Ag_3VO_4 catalysts, possessing high stability after five reaction cycles. The photocatalytic mechanism is shown in Figure 3 [24].

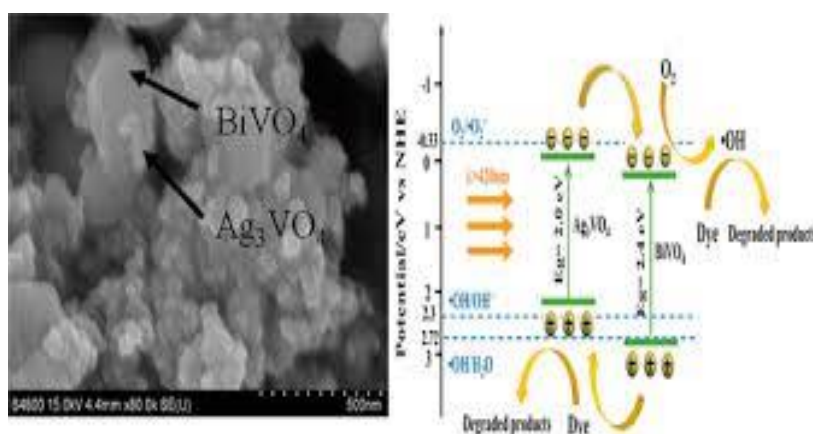


Figure 3 SEM image of $\text{BiVO}_4/\text{Ag}_3\text{VO}_4$ photocatalyst and schematic representation of its photocatalytic degradation activity [24] (Reproduced with permission).

A study regarding the decomposition of three different dyes, namely methyl orange, rhodamine B (RhB), and malachite green, was performed using a novel $\text{LaFeO}_3/\text{AgBr}$ heterojunction photocatalyst. The study revealed that the dyes were decomposed more effectively than TC [64]. Xu et al. [65] studied the visible-light-enhanced photocatalytic performance of $\text{ZnO}/\text{Cu}_2\text{O}$ compound catalyst upon degradation of methyl orange (MO), which was attributed to augmented visible light absorption and the heterostructure, resulting in enhanced dissociation of photo-liberated electrons/holes pairs in $\text{ZnO}/\text{Cu}_2\text{O}$ heterostructures. A donor-acceptor combined polymer, poly(1,3,4-oxadiazole)s (POD), was invented by Ran et al. [66] to investigate the effect of photocatalytic deterioration upon methyl orange, methylene blue, and reactive brilliant blue. The superoxide anion radical ($\text{O}_2^{\cdot-}$), along with $\cdot\text{OH}$, evolution from $\text{O}_2^{\cdot-}$ by adding H^+ , resulted in fast decomposition of the dyes. Shaban et al. [67] prepared $\text{MCM-48}/\text{Ni}_2\text{O}_3$ composite for effective photodecomposition of Congo red dye molecules, where MCM-48 acted as catalyst support for nickel oxide photocatalyst. Incorporating the Ni_2O_3 particles over the mesoporous surface of MCM-48 revealed more adsorption and photocatalytic sites for the incident light photons, resulting in an enhanced photo removal rate compared to Ni_2O_3 and MCM-48, respectively.

3.2 Phenolic Compounds

Phenol and its derivatives are moderately water-soluble contaminants commonly found in industrial wastewater, such as petroleum, paint, paper, and pharmaceutical industries. Such toxic components harm every living organism and are biologically recalcitrant [68]. Photocatalysis is the most effective process for degrading phenolic constituents from aqueous media. When the photocatalytic mechanism occurs, the principal reaction occurs in the bulk liquid, where the reactions between hydroxyl radicals present throughout the cyclic carbon liberate several oxidation products, such as hydroquinone, catechol, and p-benzoquinone. The intermediate products of the reaction, such as chlorohydroquinone, 4-chlorocatechol, and resorcinol, are transformed into acetylene, maleic acid, carbon monoxide, and carbon dioxide [2].

Moradi et al. [69] designed a FeTiO₃/GO nanocomposite through ultrasound. This, revealed much higher efficiency in removing phenolic compounds from wastewater at a pH of 8, even after five cycles, showing good recyclability. Also, it was observed that the phenol removal efficiency increased to 73%, with enhancement in the dose of the photocatalyst, but decreased with enhancement in phenol concentrations. TiO₂ nanoparticles loaded with 0.33 wt.% of reduced graphene oxide (rGO) showed an average removal percentage of 59.5% of three phenolic compounds, namely, phenol, p-chlorophenol, and p-nitrophenol analogous to 3.87 mg of reduced phenolic components under visible light irradiation. Here, rGO acted as an electron acceptor preventing the electron-hole coalescence process, thus improving the photocatalytic efficiency of TiO₂. On the other hand, the C = C combined bonds in the rGO put out the photocatalytic performance of TiO₂ to the visible light range, thereby enhancing the phenolic compounds' removal efficiencies [70]. Li et al. [71] synthesized Au-incorporated TiO₂/Fe₂O₃ heterojunction photocatalyst prepared via the metal-organic framework (MOF) technique. The study revealed exceptional photodegradation of 2,4 dichlorophenol (2,4-DCP) up to 95% and 4-bromophenol (4-B,P) up to 97% upon irradiation in visible light for 90 min and 60 min, respectively. Here, Au, possessing low resistance values, acted as an effective electron mediator to boost the transport of electrons between the Fe₂O₃ and TiO₂ interface, resulting in much better removal of phenolic compounds. Soori et al. [72] prepared a photocatalyst, where copper oxide (CuO) was supported on clinoptilolite nanoparticles (NC), for effective removal of 2,6-dimethylphenol (DMP) from wastewater at pH 5.5. The study showed an enhancement in the decomposition rate when the dose of the photocatalyst was limited to 0.1 to 0.25 g L⁻¹, but afterward, the decomposition rate was found to have decreased. Investigation upon removal of phenol was carried out using ZnO nanosheets/montmorillonite photocatalyst by Ye et al. [73], which showed maximum decomposition effectivity of 88.5% after 240 min at a 10 mg/L phenol concentration.

4. Removal of Heavy Metal Ions

The presence of heavy metal ions on the surface, as well as underground water, has been increasing very rapidly due to rising industrial effluents coming from different industries, such as the battery, mining industry, rayon industry, tanning industry, metal smelting industry, petrochemicals, and electrolysis applications [74, 75]. Heavy metal ions play a significant role in human metabolism, but an increase in the concentration of such ions is fatal for human health. In the human body, these metal ions accumulate and inhibit the normal functioning of vital body organs and glands such as the heart, brain, kidneys, bone, liver, etc. Also, they supplant the essential

mineral components from their native place, thereby obstructing their biological activity [76, 77]. Therefore, it is desirable to do away with such toxic and hazardous substances present in wastewater, before consumption or for other purposes.

4.1 Chromium (Cr)

Chromium is a familiar pollutant often found in the discharges from electroplating, pigments, and chromate industries. They appear carcinogenic and greatly threaten humans and other aquatic organisms [78]. Since the toxicity value of Cr(VI) is very high than that of Cr(III), Cr(VI) is normally converted to Cr(III) and is subsequently removed by following the technique of adsorption or precipitation [79, 80]. But secondary pollution may occur during such processes due to reductants' addition. Therefore, the evolution of a productive and eco-friendly process for eliminating Cr(VI) is necessary. The photocatalysis process appears to be an ideal option for treating Cr(VI) in water due to possessing several edges, such as non-utilization of chemical reagents, innocuous, good selectivity, and high effectivity.

Zhong et al. [81] developed a suitable technique for manufacturing flexible membranes of electro-spun carbon nanofibre/tin(IV) sulfide (CNF@SnS₂) core/sheath fibers. This newly synthesized photocatalyst provided excellent cycling stability and is highly effective for reducing Cr(VI). The CNF@SnS₂ membranes exhibited a high decomposition rate of 250 mg/L aqueous Cr(VI) and could completely remove Cr(VI) under 90 min after three cycles. The photocatalytic degradation of Cr(VI) was investigated upon BiOBr-Bi₂S₃ heterojunction photocatalyst by Long and his co-workers [82], which attained 100% removal of Cr(VI) in less than 12 minutes. The dissociation and deportation of the light-injured charged ions acted according to a direct Z-scheme path, resulting in efficient charge dissociation, electron deportation, and accretion, thereby improving the photocatalytic execution of the photocatalyst. Wang et al. [83] designed a magnetic Fe₃O₄@poly(m-phenylenediamine) particles (Fe₃O₄@PmPDs) nanostructure for effective reduction of Cr(VI) to harmless Cr(III) through the compression of amine, following the process of photocatalysis, resulting in chelation of Cr(III) on amino groups, under visible-light irradiation.

4.2 Lead (Pb)

Lead is the most toxic metal, often considered a primary pollutant. The presence of this metal in water bodies mainly relies on different processing industries, such as the battery industry, anti-knocking agent–tetraethyl-lead manufacturing, metal plating and finishing industry, and ceramic/glass industry [84]. Lead accumulation in the human body, beyond its permissible limit (0.05 mg/L), can create several diseases anemia, kidney malfunction, brain tissue damage, and death in severe cases. Therefore, it is necessary to primarily treat Pb²⁺ contaminated water before being discharged into the environment [85].

A heterogeneous photocatalytic system is a promising technique for treating heavy-metal-contaminated water. Bharath et al. [86] prepared hydroxyapatite (HAp) nanoparticles fabricated upon dendritic α -Fe₂O₃ nanocomposites. Following the pseudo-second-order model, the prepared photocatalyst has a Pb (II) removal capacity of 97.5% at pH 4. The photocatalytic compression of Pb (II) ions from wastewater was investigated using titania polyvinylalcohol–alginate beads (TPVAABs) as photocatalyst by Majidnia et al. [87], which revealed 98% efficiency in removing Pb (II) ions within 135 min under visible light irradiation. Such a removal process can occur for more than seven

adsorption cycles/desorption with effectivity. Complete degradation of Pb ions from aqueous lead-ethylenediaminetetraacetic acid solution (Pb-EDTA) was observed within 25 min using ZnO nanopowder under UV irradiation, which was attributed to the excellent absorption capacity of UV light by ZnO nanopowder [88].

4.3 Cadmium (Cd)

Cadmium is another toxic metal, considered a pollutant, since it is highly infective at low levels of exposure. Several industrial effluents are considered to be the main cause behind the rising levels of cadmium in water bodies, for instance, the battery industry, pigment industry, fertilizer industry, and coating and plating industries [89]. Once absorbed by the human body, Cd mainly accumulates in the kidney, especially in the proximal tubular cells. Consequently, excess Cd absorption by the human body can also create diseases like bone demineralization and lung cancer [90].

In the past few years, visible-light irradiated photocatalytic effluent treatment has gained much popularity since this technique is low-cost and effective for industrial purposes. Shen et al. [91] prepared calcium ferrite-based TiO_2 nanomaterials, which resulted in an excellent (99.02%) photocatalytic rate of decomposition of cadmium under solar irradiation. The CB potential of calcium ferrite turned out to be much more negative in comparison to the reduction potential of Cd (II), leading to the effective conversion of Cd (II) to Cd(0). A new dye-sensitized photocatalyst, Eosin Y-sensitized TiO_2 photocatalyst, was created by Chowdhury et al. [92] for effective Cd(II) decomposition in an aqueous medium, using Triethanolamine (TEOA) as a sacrificial electron donor. More than 83% of Cd (II) degradation was achieved within 3 h, for initial Cd(II) concentrations between 20 and 100 ppm, at a pH of 7.0. Titania polyvinyl alcohol-alginate beads (TPVA-ABs) were investigated to act as a photocatalyst to completely remove Cd(II) ions from wastewater, which lasted almost five cycles. Such efficiency was made possible due to TiO_2 nanoparticles in TPVA-ABs, which acted as a working photocatalyst for the removal of Cd(II) ions [93]. Salman Vandi et al. [94] designed another new photocatalyst with the help of ZnO supported on bentonite clay (as shown in Figure 4) [94]. Such a combination assisted in reducing the band gap to the UV range, which further excited ZnO under UV irradiation where the photogenerated electrons were injected into the CB of the bentonite, resulting in 79.05% degradation from Cd(II) to Cd(0) as shown in the below figure.

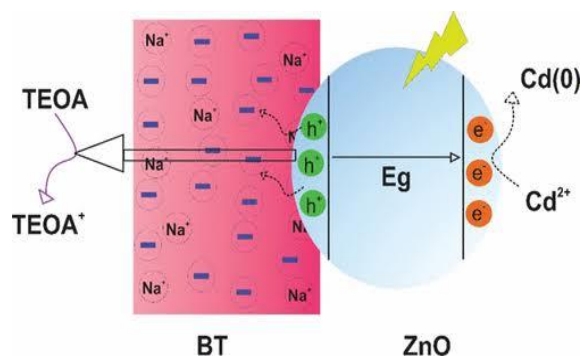


Figure 4 Schematic diagram showing the reaction process for the reduction of Cd(II) over ZnO/BT photocatalyst under solar irradiation (Reproduced with permission from [94]).

4.4 Mercury (Hg)

Mercury is a highly poisonous heavy metal, generally released into the environment from municipal sewage waste and the effluents of different industries, such as pesticides, metallurgical, electronics, pesticides, and chlor-alkali sectors [95]. Consuming water exceeding the threshold value of mercury (0.002 mg/L) may lead to developing several diseases in our body, including lung damage, brain damage, kidney diseases, and so on. Inhalation of mercury vapor or organic mercury consumption by aquatic animals may lead to Minamata disease [96]. The photocatalysis process to treat such contaminated water has gained much interest in recent years since it can reduce the pollutants in water to less toxic substances [2].

Mohamed et al. [97] investigated upon photocatalytic decomposition of Hg(II) ions from wastewater using Pd-ZnO photocatalyst fabricated upon multi-walled carbon nanotubes (MWCNT), which resulted in the complete elimination of mercury ions at a reaction time of 30 min. This excellent performance was attributed to the doping of ZnO with Pd, resulting in much lower recombination of electron-hole pairs in the photocatalyst, which was assisted by adding proper quantity of MWCNTs to the photocatalyst, thereby leading to improved photocatalytic performance of ZnO. Bamboo charcoal, possessing a large surface area, was fabricated on TiO₂ nanoparticles for efficient (95%) photocatalytic removal of Hg(II) ions at a pH of 6. In this analysis, the introduction of format acted as an organic hole scavenger, which led to the photoreduction of Hg(II) to its zero-valent form [98]. Kadi et al. [99] constructed a mesoporous α -Fe₂O₃/g-C₃N₄ Z-scheme photocatalyst, showing complete photodecomposition of Hg (II) ions in no more than 60 min of reaction time. Integrating α -Fe₂O₃ on the g-C₃N₄ surface created a redshift suitable for required charge generation in the transfer process between the VB or CB of α -Fe₂O₃ and g-C₃N₄ and the Z-scheme inhibited the rate of electrons-holes recombination, resulting in enhanced photocatalytic performance. An S-scheme heterojunction system comprising Ag₃VO₄ nanoparticles uniformly dispersed over the g-C₃N₄. The 2.4% Ag₃VO₄/C₃N₄ photocatalyst exhibited 100% photo removal of Hg (II) under 60 min, thanks to the large surface area and enhanced light absorption, indicating much effective photoinduced charge dissociation [100].

5. Removal of Pharmaceuticals

In recent years, consumption of various pharmaceuticals and personal care products (PPCPs) has risen worldwide. The byproducts generated from manufacturing such commodities are discarded in water bodies, causing water quality degradation. Consumption or domestic usage of such water creates an ill effect on human health and the environment. Various water treatment processes, such as adsorption, coagulation, flocculation, air stripping, and reverse osmosis, are very much incompetent, proving they are time-consuming and mainly chemically exhaustive processes [101]. Therefore, photocatalysis appears to be one of the most attractive technologies to treat contaminated water since it is very cost-effective and can efficiently decompose the contaminants in the water into less harmful substances [2].

5.1 Antibiotics

Among the pharmaceutical contaminants, antibiotics, mainly bactericidal and bacteriostatic drugs, are used extensively worldwide to treat several diseases. Increased consumption of this class of drugs has been found to contaminate aquatic bodies because the target organism only partially absorbs most antibiotics. Hence, the residual components are excreted through urine and feces to

reach the water bodies, creating water pollution [102, 103]. Traditional water treatment processes do not help much to remove or decompose the antibiotic contaminants from water. Photocatalysis has the potential to disintegrate those components into less toxic substances, making the water safe for general use [2].

Photocatalytic performances of the synthesized CdS/TiO₂ photocatalyst with different weights of CdS under sunlight shown in Figure 5 [67]. Tetracycline (TC) is among the top two commonly used antibiotics worldwide, which works over a wide range of bacterial infections and generally resides in soil, groundwater, and drinking water [104]. A Z-scheme Ag₃PO₄/Co₃(PO₄)₂@Ag photocatalyst was designed for the degradation of TC, which displayed much better performance than the individual nanocatalysts, having the highest rate constant of 0.034 min⁻¹. Here, introducing Ag nanoparticles enhanced the liberation of ·O₂⁻ and ·OH⁻ under solar irradiation, further improving photocatalytic efficiency [105]. A Ti-doped MCM-41 photocatalyst showed almost complete photodecomposition of oxytetracycline (OTC) under 150 mins, which was attributed to the high adsorption potential of MCM-41, leading to much better removal rate of OTC than other photocatalysts [106]. Bobirica et al. [107] synthesized a new type of photocatalyst depending upon (PLA)/TiO₂ hybrid nanofibers fabricated on fiberglass supports for effective decomposition of Ampicillin (AMP) antibiotic. However, the photodegradation rate relied upon the photocatalytic membrane used, where the best performance achieved by fiberglass fabric plain woven-type membrane resulted in 100% removal of AMP within 30 min. Wang et al. [108] developed CdS-TiO₂ nanostructure, via a novel process, which exhibited superb photocatalytic activity to decompose penicillin G (PG) under solar irradiation as shown in the Figure 5 [67].

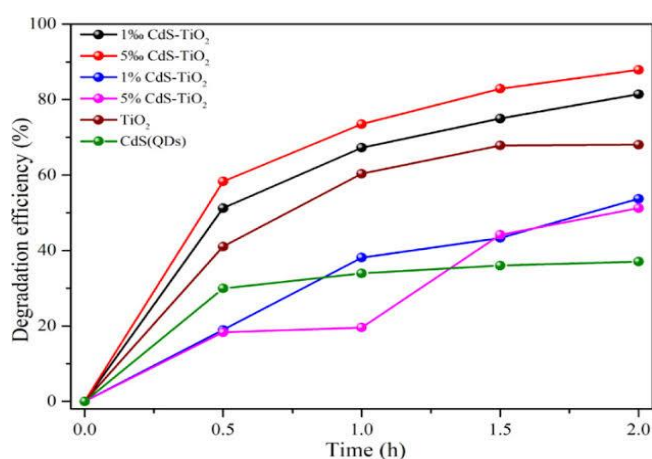


Figure 5 Schematic diagram showing photocatalytic performances of the synthesized CdS/TiO₂ photocatalyst with different weights of CdS under sunlight [67] (Reproduced with permission).

A significant contribution was made by the heterojunction nanostructure of the photocatalyst, which was successful enough to subdue the electron-hole recombination rate. The development of GO@Fe₃O₄/ZnO/SnO₂ photocatalyst to carry out the photodegradation of azithromycin in an aqueous solution was done, which displayed pH-dependent reaction efficiency. The photocatalytic efficiency was also found to remain intact after cycles [109]. A direct Z scheme 2D/2D heterojunction in the form of a Fe₃O₄/Bi₂WO₆ photocatalyst was analyzed upon removal of CIP from wastewater (See Figure 6) [110]. The result showed complete removal of CIP within a short time, which could

be ascribed to the significant effect created by superoxide radical ($\cdot\text{O}_2^-$) and hydroxyl radical ($\cdot\text{OH}$) [110].

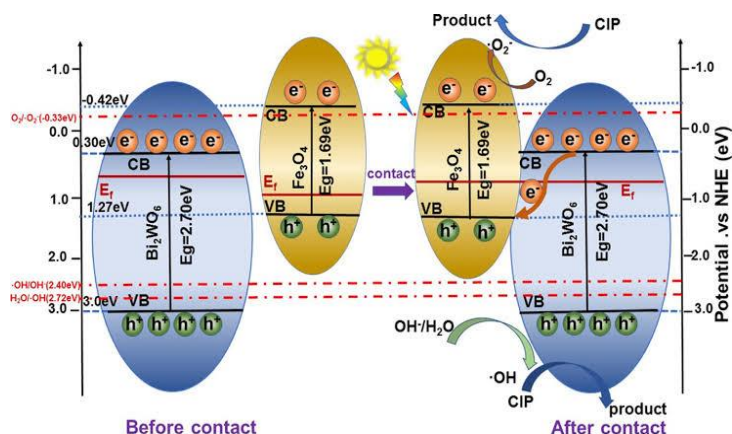


Figure 6 Photocatalytic mechanism of Z-scheme $\text{Fe}_3\text{O}_4/\text{Bi}_2\text{WO}_6$ heterojunction towards the degradation of ciprofloxacin in water (Reproduced with permission from [110]).

Kumar et al. [111] designed a hybrid $\text{Ag}_2\text{S}/\text{Bi}_2\text{S}_3/\text{g-C}_3\text{N}_4$ heterojunction photocatalyst, which was observed to degrade 97.4% of sulfamethoxazole within 90 min in the presence of visible light. The catalyst was also stable and could be reused effectively for several cycles.

5.2 Anti-Inflammatories

Anti-Inflammatory drugs exhibit a high-octanol partition coefficient, possessing a high potential to passively spread across biological membranes, making them easy to survive in soil and aquatic environments. The presence of such contaminants creates pollution of water resources. Diclofenac, ibuprofen, and naproxen are among water bodies' top three persistent pollutants [112]. The human body excretes them into water bodies, hampering different aquatic animals' lives. Wang et al. [113] developed a novel $\text{g-C}_3\text{N}_4/\text{Bi}_2\text{WO}_6$ heterojunction (UTCb) photocatalyst, which successfully removed ibuprofen (IBF) from wastewater. The development of ultrathin heterojunctions embracing effectual transfer of charge over the heterojunction terminal was the major factor contributing to efficient photocatalytic performance under sunlight. The development of $\text{ZnO}/\text{Ag}_2\text{CO}_3/\text{Ag}_2\text{O}$ photocatalyst has led to the complete mineralization of diclofenac (DCF) solution, having ten times higher photocatalytic performance than ZnO . The photocatalyst's heterojunction nanostructure has led to excellent light absorption, unlike Ag_2CO_3 and Ag_2O , which have poor light absorption characteristics [114]. Residues of naproxen (NPX), a member of the family of nonsteroidal anti-inflammatory drugs (NSAID) are often found in water bodies, affecting many lives. Ray et al. [115] have led to the creation of $\text{AgBr-}\alpha\text{-NiMoO}_4$ photocatalyst, which was able to degrade NPX about two times more efficiently than that of AgBr alone. Additionally, the photocatalyst exhibited photochemical stability.

5.3 Lipid –Regulators

Lipid regulators or antihyperlipidemic agents are commonly used to lower the lipid level, such as cholesterol in the blood. Contamination of water bodies with such complex compounds may hamper aquatic living organisms [116]. Bezafibrate (BZA), a lipid-lowering drug, was found to be effectively removed by PVA/TiO₂ photocatalyst at an optimum pH of 6.9 [117]. One of the most commonly used antidiabetic drugs, metformin, was observed to be entirely decomposed within 60 min using poly (3,4- ethylene dioxythiophene) (PEDOT) polymer under UV exposure. This performance was found to have decreased with the incorporation of various scavengers [118].

6. Pesticides

The application of pesticides is generally limited in the agricultural field to protect crops from several disease-causing biological agents such as bacteria and fungi, thereby enhancing the production rate of different crops. However, excess usage of such pesticides would lead to soil and water pollution. Additionally, many pesticides appear mutagenic and carcinogenic, which tend to damage the nerve and endocrine of the human body systems, even in low concentrations, thereby hampering the ecological balance [119, 120]. Photocatalysis has emerged as a leading technology to degrade such complex compounds effectively into harmless components such as H₂O and CO₂.

Monocrotophos, a very toxic pesticidal component, was successfully photo decomposed into small compounds within 75 mins of reaction time by a synthesized Cu-ZnO photocatalyst. Here, the Cu dopant assisted in lowering the band gap, leading to improved dissociation of photo-induced charged ions of the ZnO [121]. Removal of chlorpyrifos pesticide from aqueous solution was investigated upon nano hydroxide apatite fabricated carboxyl functionalized graphene oxide (GO)/zinc oxide (ZnO) nanorod (nHAP@CFGO/ZnR) nanocatalyst. The analysis revealed maximum photo removal capacity at a pH value of 3.5 following first-order kinetics, where CFGO assisted in faster pesticide degradation than GO [122]. To effectively decompose imidacloprid, a toxic pesticide, Soltani-nezhad and his co-workers [123] prepared TiO₂-NiO magnetic photocatalyst supported on graphene oxide nanosheets, which was proved to be beneficial to remove 5 ppm of imidacloprid pesticide at pH = 9 under visible light radiation. Mirmasoomi et al. [124] synthesized TiO₂/Fe₂O₃ nanocomposite for the removal of diazinon, where doping of Fe₂O₃ on the surface of TiO₂ helped reach the photo absorption span not only to the visible light region but also to UV light region.

7. Herbicides

Herbicides are chemical agents useful to restrict the growth of unwanted plants, such as residential or agricultural weeds and invasive species, thereby enhancing crop production worldwide with reduced cost of production [125]. Despite having several advantages, its major drawback resides in groundwater contamination through leaching. Moreover, runoff is also considered one of the principal routes of herbicide conveyance outside agricultural fields and creating water pollution [126]. These substances are very much resistant to traditional water treatment methods. Therefore, photocatalysis technology appeared suitable for removing these contaminants due to possessing cogent oxidizing and mineralizing proficiencies towards organic substances.

Xu et al. [127] conducted experiments upon $\text{H}_3\text{PW}_{12}\text{O}_{40}/\text{Ag-TiO}_2$ photocatalyst to remove atrazine (AT) herbicide from water, resulting in high photocatalytic decomposition efficiency at an initial concentration of 5 mg L^{-1} . Incorporating Ag nanoparticles might help in the deception of photogenerated electrons to intensify electron-hole separation and hand over the trapped electrons to the O_2 adsorbed onto the exterior part of the catalyst, leading to enhanced photocatalytic performance. CeO_2 nanoparticles observed fast decomposition of glyphosate within 20 mins at a pH of 4, where citric acid commenced the transfer of electrons to facilitate the resurgence of Ce^{3+} sites as electron donors and help in elevated photocatalytic performance following ligand-to-metal charge transfer [128]. Maya-Treviño et al. [129] tried to assess the performance of $\text{ZnO-Fe}_2\text{O}_3$ photocatalyst under solar light on the degradation of Dicamba and 2,4-D herbicides. The study revealed 100% decomposition of both the chemical agents, with the formation of oxalic, formic, and acetic acids as byproducts. In comparison to such conventional photocatalysts, $\text{Cu-TiO}_2/\text{SBA}_{15}$ catalyst resulted in the highest removal of paraquat herbicide under visible light irradiation at a very low pH value, where the mesoporous SBA-15 helped in enhanced surface area of TiO_2 , leading to much better photocatalytic performance of the catalyst [130].

8. Insecticides

The sole purpose of insecticides is to keep a check on the insect population in the agricultural field by killing them or preventing them from engaging in undesirable or destructive behaviors. Extensive use of such chemical agents has led to rising pollution of water bodies since they are very much stable and highly toxic. Conventional water treatment methods are unable to remove them completely [131]. Photocatalytic treatment of insecticides can be decomposed into non-toxic and easily degradable products under sunlight.

Li *et al.* [132] investigated upon the removal of a toxic insecticidal component, carbofuran, from the water following the process of photocatalysis, using a Z-scheme $\text{NaNbO}_3\text{-Au-Sn}_3\text{O}_4$ nanostructured photocatalyst, where gold nanoparticles played a significant role in the deportation of electrons. The analysis revealed an excellent photocatalytic decomposition rate of carbofuran under solar-light irradiation in not more than 120 min. Photoreduction of methomyl insecticide in water was observed by Pookmanee and his co-workers [133] using GO/BiVO_4 nanocomposite, which displayed the highest photo removal efficiency of methomyl at 200°C for 3 h. Sun et al. [134] researched a novel technique for preparing MCN450/HPW photocatalyst, developed by calcinating carbon nitride (CN) at 450°C with formaldehyde along with the introduction of tungstophosphoric acid (HPW) for the decomposition of two typical insecticides, Imidacloprid and Acetamiprid. The results showed a much better removal rate constant of imidacloprid and acetamiprid, about 6.4 and 11 times, respectively, than that of the respective nanocatalysts. Ethiofencarb, a virulent insecticide, was found to get obliterated from the water, with the help of stannum indium sulfide (SnIn_4S_8) semiconductor photocatalyst, along with the production of nine byproducts. However, inorganic anions, for example, Cl^- and NO_3^- inhibit the photodegradation process [135].

9. Conclusive Remarks

This review discussed photocatalysis which emerged as a promising technology for wastewater treatment due to its effectiveness in degrading organic pollutants and disinfecting water. Recent developments in photocatalytic applications for wastewater treatment include:

Photocatalysts: Traditional photocatalysts like titanium dioxide (TiO₂) are primarily active under ultraviolet (UV) light, which accounts for only a small portion of solar radiation. Recent efforts have focused on developing visible light-responsive photocatalysts, such as metal sulfides, carbon nitride, and perovskite-based materials. These materials can utilize a broader range of the solar spectrum, making them more energy-efficient and cost-effective [136, 137].

Advanced Photocatalytic Materials: Researchers have developed novel photocatalytic materials with enhanced properties. For example, using metal-organic frameworks (MOFs), graphene-based materials, and hybrid composites has improved photocatalytic activity, stability, and selectivity [138, 139].

Photocatalytic Membrane Reactors: Integration of photocatalysts with membranes has gained attention in recent years. Photocatalytic membrane reactors (PMRs) offer the advantage of simultaneous pollutant degradation and separation. They combine the catalytic properties of photocatalysts with the filtration capabilities of membranes, allowing efficient removal of pollutants and potential reuse of treated water.

Photocatalytic Degradation of Emerging Contaminants: Emerging contaminants such as pharmaceuticals, personal care products, and endocrine-disrupting compounds pose significant challenges to conventional wastewater treatment methods. Photocatalysis has shown promise in the degradation of these persistent organic pollutants. Researchers are exploring the mechanisms and optimizing photocatalytic systems to efficiently remove emerging contaminants.

Photocatalytic Disinfection: Photocatalytic materials can also be utilized for water disinfection by inactivating harmful microorganisms. Recent studies have investigated using photocatalysts to kill bacteria, viruses, and other pathogens. This application is particularly important for the treatment of waterborne diseases and the prevention of waterborne infections.

Scaling-Up Photocatalytic Systems: While photocatalysis has shown great potential at the laboratory scale, scaling up the technology for practical applications remains challenging. Recent developments focus on reactor design, optimization of catalyst loading, and the development of continuous-flow systems to enhance the efficiency and scalability of photocatalytic wastewater treatment.

Integration with Other Treatment Technologies: To address the complexity and diversity of pollutants in wastewater, researchers are exploring the integration of photocatalysis with other treatment technologies. Hybrid systems combining photocatalysis with adsorption, dielectric metal audition ozonation, electrochemical treatment, and biological treatment have been investigated to achieve synergistic effects and improve overall treatment efficiency [140]. These recent developments in photocatalytic applications for wastewater treatment hold great promise for addressing water pollution challenges and promoting sustainable water management practices. Ongoing research and technological advancements are expected to further optimize the efficiency, stability, and cost-effectiveness of photocatalytic systems for large-scale implementation.

Despite significant advancements in the development of photocatalysts in recent years, the efficiency of removing contaminants and the recyclability of the photocatalysts remain low. It

cannot be applied for commercial purposes. Every stride of the photocatalytic mechanism, including photogenerated charge generation, dissociation, conveyance, adsorption, and surface reaction of the semiconductor, has a remarkable influence on photocatalytic efficiency. Additionally, the execution of the catalyst, the deterioration concentration, pH, temperature, the charged nature of the contaminant, the reactor, and the light source all acted excellently to achieve the desired efficiency. It is essential to observe and consider all the factors mentioned earlier while designing and developing semiconductor photocatalysts for photocatalytic treatment of contaminants in wastewater. Additionally, a comprehensive study of the byproducts generated from the degradation processes is necessary to understand the reaction mechanism, learn about the effects of various factors, and run the reaction process effectively while following optimal conditions.

Author Contributions

P.D. - Conceptualized the work, collected data and contributed to the preparation, writing editing and proof-reading of the manuscript. S.R. supervised, conceive the idea, writing, editing the complete work and prepared the final version of the manuscript.

Competing Interests

The authors have declared that no competing interest exist.

References

1. Lee SY, Park SJ. TiO₂ photocatalyst for water treatment applications. *J Ind Eng Chem.* 2013; 19: 1761-1769.
2. Ren G, Han H, Wang Y, Liu S, Zhao J, Meng X, et al. Recent advances of photocatalytic application in water treatment: A review. *Nanomaterials.* 2021; 11: 1804.
3. Sinar Mashuri SI, Ibrahim ML, Kasim MF, Mastuli MS, Rashid U, Abdullah AH, et al. Photocatalysis for organic wastewater treatment: From the basis to current challenges for society. *Catalysts.* 2020; 10: 1260.
4. Ali NS, Kalash KR, Ahmed AN, Albayati TM. Performance of a solar photocatalysis reactor as pretreatment for wastewater via UV, UV/TiO₂, and UV/H₂O₂ to control membrane fouling. *Sci Rep.* 2022; 12: 16782.
5. Onorato C, Banasiak LJ, Schäfer AI. Inorganic trace contaminant removal from real brackish groundwater using electro dialysis. *Sep Purif Technol.* 2017; 187: 426-435.
6. Tang X, Xie B, Chen R, Wang J, Huang K, Zhu X, et al. Gravity-driven membrane filtration treating manganese-contaminated surface water: Flux stabilization and removal performance. *Chem Eng J.* 2020; 397: 125248.
7. Reyes-Serrano A, López-Alejo JE, Hernández-Cortázar MA, Elizalde I. Removing contaminants from tannery wastewater by chemical precipitation using CaO and Ca(OH)₂. *Chin J Chem Eng.* 2020; 28: 1107-1111.
8. Yagub MT, Sen TK, Afroze S, Ang HM. Dye and its removal from aqueous solution by adsorption: A review. *Adv Colloid Interface Sci.* 2014; 209: 172-184.

9. Moussavi G, Hosseini H, Alahabadi A. The investigation of diazinon pesticide removal from contaminated water by adsorption onto NH_4Cl -induced activated carbon. *Chem Eng J.* 2013; 214: 172-179.
10. Albayati TM, Doyle AM. SBA-15 supported bimetallic catalysts for enhancement isomers production during n-heptane decomposition. *Int J Chem React Eng.* 2014; 12: 345-354.
11. Alardhi SM, Albayati TM, Alrubaye JM. Adsorption of the methyl green dye pollutant from aqueous solution using mesoporous materials MCM-41 in a fixed-bed column. *Heliyon.* 2020; 6: e03253.
12. Mousset E, Doudrick K. A review of electrochemical reduction processes to treat oxidized contaminants in water. *Curr Opin Electrochem.* 2020; 22: 221-227.
13. Widiasa IN, Wenten IG. Removal of inorganic contaminants in sugar refining process using electrodeionization. *J Food Eng.* 2014; 133: 40-45.
14. Arar Ö, Yüksel Ü, Kabay N, Yüksel M. Various applications of electrodeionization (EDI) method for water treatment—A short review. *Desalination.* 2014; 342: 16-22.
15. Elsevier Science. Photocatalysis. In: *Advanced oxidation processes for waste water treatment.* Amsterdam: Elsevier Science; 2018. pp. 135-175.
16. Abbood NS, Ali NS, Khader EH, Majdi HS, Albayati TM, Saady NM. Photocatalytic degradation of cefotaxime pharmaceutical compounds onto a modified nanocatalyst. *Res Chem Intermed.* 2023; 49: 43-56.
17. Low J, Yu J, Jaroniec M, Wageh S, Al-Ghamdi AA. Heterojunction photocatalysts. *Adv Mater.* 2017; 29: 1601694.
18. Fu J, Yu J, Jiang C, Cheng B. g- C_3N_4 -Based heterostructured photocatalysts. *Adv Energy Mater.* 2018; 8: 1701503.
19. Jabbar ZH, Graimed BH, Issa MA, Ammar SH, Ebrahim SE, Khadim HJ, et al. Photocatalytic degradation of Congo red dye using magnetic silica-coated $\text{Ag}_2\text{WO}_4/\text{Ag}_2\text{S}$ as Type I heterojunction photocatalyst: Stability and mechanisms studies. *Mater Sci Semicond Process.* 2023; 153: 107151.
20. Kumar A, Khan M, He J, Lo IM. Recent developments and challenges in practical application of visible-light-driven TiO_2 -based heterojunctions for PPCP degradation: A critical review. *Water Res.* 2020; 170: 115356.
21. Acharya R, Parida K. A review on $\text{TiO}_2/\text{g-C}_3\text{N}_4$ visible-light-responsive photocatalysts for sustainable energy generation and environmental remediation. *J Environ Chem Eng.* 2020; 8: 103896.
22. Bhoi YP, Mishra BG. Photocatalytic degradation of alachlor using type-II $\text{CuS}/\text{BiFeO}_3$ heterojunctions as novel photocatalyst under visible light irradiation. *Chem Eng J.* 2018; 344: 391-401.
23. Li J, Chen J, Fang H, Guo X, Rui Z. Plasmonic metal bridge leading type III heterojunctions to robust type B photothermocatalysts. *Ind Eng Chem Res.* 2021; 60: 8420-8429.
24. Heng H, Gan Q, Meng P, Liu X. The visible-light-driven type III heterojunction $\text{H}_3\text{PW}_{12}\text{O}_{40}/\text{TiO}_2\text{-In}_2\text{S}_3$: A photocatalysis composite with enhanced photocatalytic activity. *J Alloys Compd.* 2017; 696: 51-59.
25. Yu C, Wu Z, Liu R, Dionysiou DD, Yang K, Wang C, et al. Novel fluorinated Bi_2MoO_6 nanocrystals for efficient photocatalytic removal of water organic pollutants under different light source illumination. *Appl Catal B.* 2017; 209: 1-11.

26. Benaissa M, Abbas N, Al Arni S, Elboughdiri N, Moumen A, Hamdy MS, et al. BiVO₃/g-C₃N₄ S-scheme heterojunction nanocomposite photocatalyst for hydrogen production and amaranth dye removal. *Opt Mater*. 2021; 118: 111237.
27. Xu Q, Zhang L, Cheng B, Fan J, Yu J. S-scheme heterojunction photocatalyst. *Chem*. 2020; 6: 1543-1559.
28. Bao Y, Song S, Yao G, Jiang S. S-scheme photocatalytic systems. *Sol RRL*. 2021; 5: 2100118.
29. Jabbar ZH, Okab AA, Graimed BH, Issa MA, Ammar SH. Photocatalytic destruction of Congo red dye in wastewater using a novel Ag₂WO₄/Bi₂S₃ nanocomposite decorated g-C₃N₄ nanosheet as ternary S-scheme heterojunction: Improving the charge transfer efficiency. *Diam Relat Mater*. 2023; 133: 109711.
30. Ren Y, Zeng D, Ong WJ. Interfacial engineering of graphitic carbon nitride (g-C₃N₄)-based metal sulfide heterojunction photocatalysts for energy conversion: A review. *Chinese J Catal*. 2019; 40: 289-319.
31. Li X, Yu Z, Shao L, Zeng H, Liu Y, Feng X. A novel strategy to construct a visible-light-driven Z-scheme (ZnAl-LDH with active phase/g-C₃N₄) heterojunction catalyst via polydopamine bridge (a similar "bridge" structure). *J Hazard Mater*. 2020; 386: 121650.
32. Wu L, Zhang L, Liu R, Ge H, Tao Z, Meng Q, et al. 2D/2D g-C₃N₄/1T-MoS₂ nanohybrids as schottky heterojunction photocatalysts for nuclear wastewater pretreatment. *ACS ES&T Water*. 2021; 1: 2197-2205.
33. Wen JQ, Xie J, Chen XB, Li X. A review on g-C₃N₄-based photocatalysts. *Appl Surf Sci*. 2017; 391: 72-123.
34. Zhang Y, Chen Z, Shi Z, Lu TT, Chen D, Wang Q, et al. A direct Z-scheme BiOBr/TzDa COF heterojunction photocatalyst with enhanced performance on visible-light driven removal of organic dye and Cr(VI). *Sep Purif Technol*. 2021; 275: 119216.
35. Jabbar ZH, Okab AA, Graimed BH, Issa MA, Ammar SH. Fabrication of g-C₃N₄ nanosheets immobilized Bi₂S₃/Ag₂WO₄ nanorods for photocatalytic disinfection of *Staphylococcus aureus* cells in wastewater: Dual S-scheme charge separation pathway. *J Photochem Photobiol A*. 2023; 438: 114556.
36. Lafta MA, Ammar SH, Khadim HJ, Jabbar ZH. Improved photocatalytic degradation of methyl violet dye and pathogenic bacteria using g-C₃N₄ supported phosphotungstic acid heterojunction. *J Photochem Photobiol A*. 2023; 437: 114506.
37. Raza W, Faisal SM, Owais M, Bahnemann D, Muneer M. Facile fabrication of highly efficient modified ZnO photocatalyst with enhanced photocatalytic, antibacterial and anticancer activity. *RSC Adv*. 2016; 6: 78335-78350.
38. Noman MT, Amor N, Petru M, Mahmood A, Kejzlar P. Photocatalytic behaviour of zinc oxide nanostructures on surface activation of polymeric fibres. *Polymers*. 2021; 13: 1227.
39. Harish S, Archana J, Sabarinathan M, Navaneethan M, Nisha KD, Ponnusamy S, et al. Controlled structural and compositional characteristic of visible light active ZnO/CuO photocatalyst for the degradation of organic pollutant. *Appl Surf Sci*. 2017; 418: 103-112.
40. Abebe B, Murthy HA, Amare E. Enhancing the photocatalytic efficiency of ZnO: Defects, heterojunction, and optimization. *Environ Nanotechnol Moni Manag*. 2020; 14: 100336.
41. Jabbar ZH, Graimed BH, Alsunbuli MM, Sabit DA. Developing a magnetic bismuth-based quaternary semiconductor boosted by plasmonic action for photocatalytic detoxification of

- Cr(VI) and norfloxacin antibiotic under simulated solar irradiation: Synergistic work and radical mechanism. *J Alloys Compd.* 2023; 958: 170521.
42. Graimed BH, Okab AA, Jabbar ZH, Issa MA, Ammar SH. Highly stable β -Bi₂O₃/Ag decorated nanosilica as an efficient Schottky heterojunction for ciprofloxacin photodegradation in wastewater under LED illumination. *Mater Sci Semicond Process.* 2023; 156: 107303.
 43. Jabbar ZH, Graimed BH, Okab AA, Alsunbuli MM, Al-husseiny RA. Construction of 3D flower-like Bi₅O₇/Bi/Bi₂WO₆ heterostructure decorated NiFe₂O₄ nanoparticles for photocatalytic destruction of Levofloxacin in aqueous solution: Synergistic effect between S-scheme and SPR action. *J Photochem Photobiol A.* 2023; 441: 114734.
 44. Xie T, Hu J, Yang J, Liu C, Xu L, Wang J, et al. Visible-light-driven photocatalytic activity of magnetic BiOBr/SrFe₁₂O₁₉ nanosheets. *Nanomaterials.* 2019; 9: 735.
 45. Maisang W, Phuruangrat A, Randorn C, Kungwankunakorn S, Thongtem S, Wiranwetchayan O, et al. Enhanced photocatalytic performance of visible-light-driven BiOBr/BiPO₄ composites. *Mater Sci Semicond Process.* 2018; 75: 319-326.
 46. Sabit DA, Ebrahim SE, Jabbar ZH. Immobilization of 0D CuO/ZnFe₂O₄ nanoparticles onto 2D BiOBr nanoplates as dual S-scheme heterostructure for boosting photocatalytic oxidation of levofloxacin in wastewater: Magnetic reusability and mechanism insights. *J Photochem Photobiol A.* 2023; 443: 114849.
 47. Wang K, Zhan S, Zhang D, Sun H, Jin X, Wang J. Three-dimensional graphene encapsulated Ag-ZnFe₂O₄ flower-like nanocomposites with enhanced photocatalytic degradation of enrofloxacin. *RSC Adv.* 2021; 11: 4723-4739.
 48. Sharma S, Dutta V, Raizada P, Hosseini-Bandegharai A, Thakur V, Nguyen VH, et al. An overview of heterojunctioned ZnFe₂O₄ photocatalyst for enhanced oxidative water purification. *J Environ Chem Eng.* 2021; 9: 105812.
 49. Duan J, Liu M, Song X, Wang W, Zhang Z, Li C. Enhanced photocatalytic degradation of organic pollutants using carbon nanotube mediated CuO and Bi₂WO₆ sandwich flaky structures. *Nanotechnology.* 2020; 31: 425202.
 50. Chauhan A, Sharma M, Kumar S, Thirumalai S, Kumar RV, Vaish R. TiO₂@C core@shell nanocomposites: A single precursor synthesis of photocatalyst for efficient solar water treatment. *J Hazard Mater.* 2020; 381: 120883.
 51. Abdel-Wahed MS, El-Kalliny AS, Badawy MI, Attia MS, Gad-Allah TA. Core double-shell MnFe₂O₄@rGO@TiO₂ superparamagnetic photocatalyst for wastewater treatment under solar light. *Chem Eng J.* 2020; 382: 122936.
 52. Wetchakun N, Chainet S, Phanichphant S, Wetchakun K. Efficient photocatalytic degradation of methylene blue over BiVO₄/TiO₂ nanocomposites. *Ceram Int.* 2015; 41: 5999-6004.
 53. Ameta R, Benjamin S, Ameta A, Ameta SC. Photocatalytic degradation of organic pollutants: A review. *Mater Sci Forum.* 2012; 734: 247-272.
 54. Aksu Z. Application of biosorption for the removal of organic pollutants: A review. *Process Biochem.* 2005; 40: 997-1026.
 55. Xia T, Lin Y, Li W, Ju M. Photocatalytic degradation of organic pollutants by MOFs based materials: A review. *Chin Chem Lett.* 2021; 32: 2975-2984.
 56. Wang CC, Li JR, Lv XL, Zhang YQ, Guo G. Photocatalytic organic pollutants degradation in metal-organic frameworks. *Energy Environ Sci.* 2014; 7: 2831-2867.

57. Paumo HK, Dalhatou S, Katata-Seru LM, Kamdem BP, Tijani JO, Vishwanathan V, et al. TiO₂ assisted photocatalysts for degradation of emerging organic pollutants in water and wastewater. *J Mol Liq.* 2021; 331: 115458.
58. Samarghandi MR, Yang JK, Lee SM, Giahi O, Shirzad-Siboni M. Effect of different type of organic compounds on the photocatalytic reduction of Cr(VI) in presence of ZnO nanoparticles. *Desalination Water Treat.* 2014; 52: 1531-1538.
59. Stelo F, Kublik N, Ullah S, Wender H. Recent advances in Bi₂MoO₆ based Z-scheme heterojunctions for photocatalytic degradation of pollutants. *J Alloys Compd.* 2020; 829: 154591.
60. Koiki BA, Arotiba OA. Cu₂O as an emerging semiconductor in photocatalytic and photoelectrocatalytic treatment of water contaminated with organic substances: A review. *RSC Adv.* 2020; 10: 36514-36525.
61. Zhu T, Chen JS, Lou XW. Highly efficient removal of organic dyes from waste water using hierarchical NiO spheres with high surface area. *J Phys Chem C.* 2012; 116: 6873-6878.
62. Vaiano V, Sannino D, Sacco O. Heterogeneous photocatalysis: How doping with nitrogen can improve the performance of semiconductor nanoparticles under visible light irradiation. In: *Nanomaterials for the detection and removal of wastewater pollutants.* Amsterdam: Elsevier Science; 2020. pp. 285-301.
63. Yan M, Wu Y, Yan Y, Yan X, Zhu F, Hua Y, et al. Synthesis and characterization of novel BiVO₄/Ag₃VO₄ heterojunction with enhanced visible-light-driven photocatalytic degradation of dyes. *ACS Sustain Chem Eng.* 2016; 4: 757-766.
64. Song Y, Xue S, Wang G, Jin J, Liang Q, Li Z, et al. Enhanced photocatalytic decomposition of an organic dye under visible light with a stable LaFeO₃/AgBr heterostructured photocatalyst. *J Phys Chem Solids.* 2018; 121: 329-338.
65. Xu C, Cao L, Su G, Liu W, Liu H, Yu Y, et al. Preparation of ZnO/Cu₂O compound photocatalyst and application in treating organic dyes. *J Hazard Mater.* 2010; 176: 807-813.
66. Ran X, Duan L, Chen X, Yang X. Photocatalytic degradation of organic dyes by the conjugated polymer poly(1,3,4-oxadiazole)s and its photocatalytic mechanism. *J Mater Sci.* 2018; 53: 7048-7059.
67. Shaban M, Hamd A, Amin RR, Abukhadra MR, Khalek AA, Khan AA, et al. Preparation and characterization of MCM-48/nickel oxide composite as an efficient and reusable catalyst for the assessment of photocatalytic activity. *Environ Sci Pollut Res.* 2020; 27: 32670-32682.
68. Raza W, Lee J, Raza N, Luo Y, Kim KH, Yang J. Removal of phenolic compounds from industrial waste water based on membrane-based technologies. *J Ind Eng Chem.* 2019; 71: 1-8.
69. Moradi M, Vasseghian Y, Khataee A, Harati M, Arfaeina H. Ultrasound-assisted synthesis of FeTiO₃/GO nanocomposite for photocatalytic degradation of phenol under visible light irradiation. *Sep Purif Technol.* 2021; 261: 118274.
70. Al-Kandari H, Abdullah AM, Mohamed AM, Al-Kandari S. Enhanced photocatalytic degradation of a phenolic compounds' mixture using a highly efficient TiO₂/reduced graphene oxide nanocomposite. *J Mater Sci.* 2016; 51: 8331-8845.
71. Li Y, Yang B, Liu B. MOF assisted synthesis of TiO₂/Au/Fe₂O₃ hybrids with enhanced photocatalytic hydrogen production and simultaneous removal of toxic phenolic compounds. *J Mol Liq.* 2021; 322: 114815.

72. Soori F, Nezamzadeh-Ejhieh A. Synergistic effects of copper oxide-zeolite nanoparticles composite on photocatalytic degradation of 2,6-dimethylphenol aqueous solution. *J Mol Liq.* 2018; 255: 250-256.
73. Ye J, Li X, Hong J, Chen J, Fan Q. Photocatalytic degradation of phenol over ZnO nanosheets immobilized on montmorillonite. *Mater Sci Semicond Process.* 2015; 39: 17-22.
74. Zhou Q, Yang N, Li Y, Ren B, Ding X, Bian H, et al. Total concentrations and sources of heavy metal pollution in global river and lake water bodies from 1972 to 2017. *Glob Ecol Conserv.* 2020; 22: e00925.
75. Kinuthia GK, Ngure V, Beti D, Lugalia R, Wangila A, Kamau L. Levels of heavy metals in wastewater and soil samples from open drainage channels in Nairobi, Kenya: Community health implication. *Sci Rep.* 2020; 10: 8434.
76. Rehman K, Fatima F, Waheed I, Akash MS. Prevalence of exposure of heavy metals and their impact on health consequences. *J Cell Biochem.* 2018; 119: 157-184.
77. Fu Z, Xi S. The effects of heavy metals on human metabolism. *Toxicol Mech Methods.* 2020; 30: 167-176.
78. Zhang YC, Yao L, Zhang G, Dionysiou DD, Li J, Du X. One-step hydrothermal synthesis of high-performance visible-light-driven SnS₂/SnO₂ nanoheterojunction photocatalyst for the reduction of aqueous Cr(VI). *Appl Catal B.* 2014; 144: 730-738.
79. Du XD, Yi XH, Wang P, Zheng W, Deng J, Wang CC. Robust photocatalytic reduction of Cr(VI) on UiO-66-NH₂(Zr/Hf) metal-organic framework membrane under sunlight irradiation. *Che Eng J.* 2019; 356: 393-399.
80. Deng F, Lu X, Luo Y, Wang J, Che W, Yang R, et al. Novel visible-light-driven direct Z-scheme CdS/CuInS₂ nanoplates for excellent photocatalytic degradation performance and highly-efficient Cr(VI) reduction. *Chem Eng J.* 2019; 361: 1451-1461.
81. Zhong Y, Qiu X, Chen D, Li N, Xu Q, Li H, et al. Flexible electrospun carbon nanofiber/tin(IV) sulfide core/sheath membranes for photocatalytically treating chromium(VI)-containing wastewater. *ACS Appl Mater Interfaces.* 2016; 8: 28671-28677.
82. Long Z, Zhang G, Du H, Zhu J, Li J. Preparation and application of BiOBr-Bi₂S₃ heterojunctions for efficient photocatalytic removal of Cr(VI). *J Hazard Mater.* 2021; 407: 124394.
83. Wang T, Zhang L, Li C, Yang W, Song T, Tang C, et al. Synthesis of core-shell magnetic Fe₃O₄@poly(m-phenylenediamine) particles for chromium reduction and adsorption. *Environ Sci Technol.* 2015; 49: 5654-5662.
84. Kumar V, Wanchoo RK, Toor AP. Photocatalytic reduction and crystallization hybrid system for removal and recovery of lead(Pb). *Ind Eng Chem Res.* 2021; 60: 8901-8910.
85. Assi MA, Hezmee MN, Sabri MY, Rajion MA. The detrimental effects of lead on human and animal health. *Vet World.* 2016; 9: 660-671.
86. Bharath G, Ponpandian N. Hydroxyapatite nanoparticles on dendritic α -Fe₂O₃ hierarchical architectures for a heterogeneous photocatalyst and adsorption of Pb(II) ions from industrial wastewater. *RSC Adv.* 2015; 5: 84685-84693.
87. Majidnia Z, Fulazzaky MA. Photoreduction of Pb(II) ions from aqueous solution by titania polyvinylalcohol-alginate beads. *J Taiwan Inst Chem Eng.* 2016; 66: 88-96.
88. Park S, Park G, Byun K, Lee SH, Han MJ. Utilization of zinc oxide nanopowder for photocatalytic removal of Pb⁺⁺ ions from aqueous wastewater. *J Nanosci Nanotechnol.* 2020; 20: 6831-6834.

89. Nguyen VN, Amal R, Beydoun D. Effect of formate and methanol on photoreduction/removal of toxic cadmium ions using TiO₂ semiconductor as photocatalyst. *Chem Eng Sci.* 2003; 58: 4429-4439.
90. Thévenod F, Lee WK. Toxicology of cadmium and its damage to mammalian organs. In: *Cadmium: From toxicity to essentiality.* Dordrecht: Springer; 2013. pp. 415-490.
91. Shen Y, Xu B, Zhu S, Zhang F, Zhao Q, Li X. Enhanced photocatalytic reduction of cadmium on calcium ferrite-based nanocomposites by simulated solar radiation. *Mater Lett.* 2018; 211: 142-145.
92. Chowdhury P, Athapaththu S, Elkamel A, Ray AK. Visible-solar-light-driven photo-reduction and removal of cadmium ion with Eosin Y-sensitized TiO₂ in aqueous solution of triethanolamine. *Sep Purif Technol.* 2017; 174: 109-115.
93. Fulazzaky MA, Majidnia Z, Idris A. Mass transfer kinetics of Cd(II) ions adsorption by titania polyvinylalcohol-alginate beads from aqueous solution. *Chem Eng J.* 2017; 308: 700-709.
94. Salmanvandi H, Rezaei P, Tamsilian Y. Photoreduction and removal of cadmium ions over bentonite clay-supported zinc oxide microcubes in an aqueous solution. *ACS Omega.* 2020; 5: 13176-13184.
95. Spanu D, Bestetti A, Hildebrand H, Schmuki P, Altomare M, Recchia S. Photocatalytic reduction and scavenging of Hg(II) over templated-dewetted Au on TiO₂ nanotubes. *Photochem Photobiol Sci.* 2019; 18: 1046-1055.
96. Jayalakshmi T, Prashanth SA, Alharthi FA, Nagaraju G. Enhanced photocatalytic activity and electrochemical behaviour towards Hg(II) of CeO₂: Ag nanocomposite. *J Electron Mater.* 2020; 49: 7568-7580.
97. Mohamed RM, Salam MA. Photocatalytic reduction of aqueous mercury(II) using multi-walled carbon nanotubes/Pd-ZnO nanocomposite. *Mater Res Bull.* 2014; 50: 85-90.
98. Xia CB, Liu CH, Liu ZH, Wu DX. Photocatalytic removal of toxic Hg(II) ions using TiO₂-modified bamboo charcoal as photocatalyst. *Adv Mat Res.* 2012; 550: 2182-2185.
99. Kadi MW, Mohamed RM, Ismail AA, Bahnemann DW. Performance of mesoporous α -Fe₂O₃/g-C₃N₄ heterojunction for photoreduction of Hg(II) under visible light illumination. *Ceram Int.* 2020; 46: 23098-23106
100. Alshaikh H, Al-Hajji LA, Mahmoud MH, Ismail AA. Visible-light-driven S-scheme mesoporous Ag₃VO₄/C₃N₄ heterojunction with promoted photocatalytic performances. *Sep Purif Technol.* 2021; 272: 118914.
101. Delgado N, Capparelli A, Navarro A, Marino D. Pharmaceutical emerging pollutants removal from water using powdered activated carbon: Study of kinetics and adsorption equilibrium. *J Environ Manage.* 2019; 236: 301-308.
102. Baaloudj O, Assadi I, Nasrallah N, El Jery A, Khezami L, Assadi AA. Simultaneous removal of antibiotics and inactivation of antibiotic-resistant bacteria by photocatalysis: A review. *J Water Process Eng.* 2021; 42: 102089.
103. Martinez JL. Environmental pollution by antibiotics and by antibiotic resistance determinants. *Environ Pollut.* 2009; 157: 2893-2902.
104. Li Z, Zhu L, Wu W, Wang S, Qiang L. Highly efficient photocatalysis toward tetracycline under simulated solar-light by Ag⁺-CDs-Bi₂WO₆: Synergistic effects of silver ions and carbon dots. *Appl Catal B.* 2016; 192: 277-285.

105. Shi W, Li M, Huang X, Ren H, Guo F, Yan C. Three-dimensional Z-Scheme $\text{Ag}_3\text{PO}_4/\text{Co}_3(\text{PO}_4)_2@Ag$ heterojunction for improved visible-light photocatalytic degradation activity of tetracycline. *J Alloys Compd.* 2020; 818: 152883.
106. Zhou K, Xie XD, Chang CT. Photocatalytic degradation of tetracycline by Ti-MCM-41 prepared at room temperature and biotoxicity of degradation products. *Appl Surf Sci.* 2017; 416: 248-258.
107. Bobirică C, Bobirică L, Râpă M, Matei E, Predescu AM, Orbeci C. Photocatalytic degradation of ampicillin using PLA/ TiO_2 hybrid nanofibers coated on different types of fiberglass. *Water.* 2020; 12: 176.
108. Wang S, Liu D, Yu J, Zhang X, Zhao P, Ren Z, et al. Photocatalytic penicillin degradation performance and the mechanism of the fragmented TiO_2 modified by CdS quantum dots. *ACS Omega.* 2021; 6: 18178-18189.
109. Sayadi MH, Sobhani S, Shekari H. Photocatalytic degradation of azithromycin using $\text{GO}@Fe_3O_4/\text{ZnO}/\text{SnO}_2$ nanocomposites. *J Clean Prod.* 2019; 232: 127-136.
110. Zhu B, Song D, Jia T, Sun W, Wang D, Wang L, et al. Effective visible light-driven photocatalytic degradation of ciprofloxacin over flower-like $\text{Fe}_3\text{O}_4/\text{Bi}_2\text{WO}_6$ composites. *ACS Omega.* 2021; 6: 1647-1656.
111. Kumar A, Sharma G, Naushad M, AlOthman ZA, Dhiman P. Environmental pollution remediation via photocatalytic degradation of sulfamethoxazole from waste water using sustainable $\text{Ag}_2\text{S}/\text{Bi}_2\text{S}_3/g\text{-C}_3\text{N}_4$ nano-Hybrids. *Earth Syst Environ.* 2021; 6: 141-156.
112. Kaur A, Umar A, Kansal SK. Heterogeneous photocatalytic studies of analgesic and non-steroidal anti-inflammatory drugs. *Appl Catal A.* 2016; 510: 134-155.
113. Wang J, Tang L, Zeng G, Deng Y, Liu Y, Wang L, et al. Atomic scale $g\text{-C}_3\text{N}_4/\text{Bi}_2\text{WO}_6$ 2D/2D heterojunction with enhanced photocatalytic degradation of ibuprofen under visible light irradiation. *Appl Catal B.* 2017; 209: 285-294.
114. Rosman N, Salleh WN, Mohamed MA, Harun Z, Ismail AF, Aziz F. Constructing a compact heterojunction structure of $\text{Ag}_2\text{CO}_3/\text{Ag}_2\text{O}$ *in-situ* intermediate phase transformation decorated on ZnO with superior photocatalytic degradation of ibuprofen. *Sep Purif Technol.* 2020; 251: 117391.
115. Ray SK, Dhakal D, Lee SW. Rapid degradation of naproxen by $\text{AgBr-}\alpha\text{-NiMoO}_4$ composite photocatalyst in visible light: Mechanism and pathways. *Chem Eng J.* 2018; 347: 836-848.
116. Mimeault C, Woodhouse AJ, Miao XS, Metcalfe CD, Moon TW, Trudeau VL. The human lipid regulator, gemfibrozil bioconcentrates and reduces testosterone in the goldfish, *Carassius auratus*. *Aquat Toxicol.* 2005; 73: 44-54.
117. Ren M, Frimmel FH, Abbt-Braun G. Multi-cycle photocatalytic degradation of bezafibrate by a cast polyvinyl alcohol/titanium dioxide (PVA/TiO_2) hybrid film. *J Mol Catal A Chem.* 2015; 400: 42-48.
118. Kumar R, Akbarinejad A, Jasemizad T, Fucina R, Travas-Sejdic J, Padhye LP. The removal of metformin and other selected PPCPs from water by poly (3,4-ethylenedioxythiophene) photocatalyst. *Sci Total Environ.* 2021; 751: 142302.
119. Bao LJ, Maruya KA, Snyder SA, Zeng EY. China's water pollution by persistent organic pollutants. *Environ Pollut.* 2012; 163: 100-108.
120. Lai W. Pesticide use and health outcomes: Evidence from agricultural water pollution in China. *J Environ Econ Manage.* 2017; 86: 93-120.

121. Hanh NT, Tri NL, Van Thuan D, Tung MH, Pham TD, Minh TD, et al. Monocrotophos pesticide effectively removed by novel visible light driven Cu doped ZnO photocatalyst. *J Photochem Photobiol A*. 2019; 382: 111923.
122. Anirudhan TS, Shainy F, Sekhar VC, Athira VS. Highly efficient photocatalytic degradation of chlorpyrifos in aqueous solutions by nano hydroxyapatite modified CFGO/ZnO nanorod composite. *J Photochem Photobiol A*. 2021; 418: 113333.
123. Soltani-nezhad F, Saljooqi A, Shamspur T, Mostafavi A. Photocatalytic degradation of imidacloprid using GO/Fe₃O₄/TiO₂-NiO under visible radiation: Optimization by response level method. *Polyhedron*. 2019; 165: 188-196.
124. Mirmasoomi SR, Ghazi MM, Galedari M. Photocatalytic degradation of diazinon under visible light using TiO₂/Fe₂O₃ nanocomposite synthesized by ultrasonic-assisted impregnation method. *Sep Purif Technol*. 2017; 175: 418-427.
125. Gianessi LP. The increasing importance of herbicides in worldwide crop production. *Pest Manag Sci*. 2013; 69: 1099-1105.
126. Vela N, Fenoll J, Garrido I, Navarro G, Gambín M, Navarro S. Photocatalytic mitigation of triazinone herbicide residues using titanium dioxide in slurry photoreactor. *Catal Today*. 2015; 252: 70-77.
127. Xu L, Zang H, Zhang Q, Chen Y, Wei Y, Yan J, et al. Photocatalytic degradation of atrazine by H₃PW₁₂O₄₀/Ag-TiO₂: Kinetics, mechanism and degradation pathways. *Chem Eng J*. 2013; 232: 174-182.
128. Wu H, Sun Q, Chen J, Wang GY, Wang D, Zeng XF, et al. Citric acid-assisted ultrasmall CeO₂ nanoparticles for efficient photocatalytic degradation of glyphosate. *Chem Eng J*. 2021; 425: 130640.
129. Maya-Treviño ML, Guzmán-Mar JL, Hinojosa-Reyes L, Ramos-Delgado NA, Maldonado MI, Hernández-Ramírez A. Activity of the ZnO-Fe₂O₃ catalyst on the degradation of Dicamba and 2,4-D herbicides using simulated solar light. *Ceram Int*. 2014; 40: 8701-8708.
130. Sorolla II MG, Dalida ML, Khemthong P, Grisdanurak N. Photocatalytic degradation of paraquat using nano-sized Cu-TiO₂/SBA-15 under UV and visible light. *J Environ Sci*. 2012; 24: 1125-1132.
131. Abdelhameed RM, Abdel-Gawad H, Elshahat M, Emam HE. Cu-BTC@cotton composite: Design and removal of ethion insecticide from water. *RSC Adv*. 2016; 6: 42324-42333.
132. Li S, Liu Z, Qu Z, Piao C, Liu J, Xu D, et al. An all-solid-state Z-scheme NaNbO₃-Au-Sn₃O₄ photocatalyst for effective degradation of carbofuran under sunlight irradiation. *J Photochem Photobiol A*. 2020; 389: 112246.
133. Pookmanee P, Longchin P, Phanmalee J, Kangwansupamonkon W, Phanichphant S. Performance photocatalytic degradation of methomyl onto composite graphene oxide/bismuth vanadate (GO/BiVO₄) nanoparticle. *Key Eng. Mater*. 2017; 751: 701-706.
134. Sun Y, Liu X. Efficient visible-light photocatalytic degradation of imidacloprid and acetamiprid using a modified carbon nitride/tungstophosphoric acid composite induced by a nucleophilic addition reaction. *Appl Surf Sci*. 2019; 485: 423-431.
135. Chen CC, Shaya J, Polychronopoulou K, Golovko VB, Tesana S, Wang SY, et al. Photocatalytic degradation of ethiofencarb by a visible light-driven SnIn₄S₈ photocatalyst. *Nanomaterials*. 2021; 11: 1325.

136. Roy S, Han GS, Shin H, Lee JW, Mun J, Shin H, et al. Low temperature synthesis of rutile TiO₂ nanocrystals and their photovoltaic and photocatalytic properties. *J Nanosci Nanotechnol.* 2015; 15: 4516-4521.
137. Maitra S, Halder S, Maitra T, Roy S. Superior light absorbing CdS/vanadium sulphide nanowalls@TiO₂ nanorod ternary heterojunction photoanodes for solar water splitting. *New J Chem.* 2021; 45: 7353-7367.
138. Mishra R, Bera S, Chatterjee R, Banerjee S, Bhattacharya S, Biswas A, et al. A review on Z/S-scheme heterojunction for photocatalytic applications based on metal halide perovskite materials. *Appl Surf Sci.* 2022; 9: 100241.
139. Moyez A, Dhar A, Sarkar P, Jung HS, Roy S. A review of the multiple exciton generation in photovoltaics. *Rev Adv Sci Eng.* 2016; 5: 51-64.
140. Dey A, Karan P, Sengupta A, Moyez SA, Sarkar P, Majumder SB, et al. Enhanced charge carrier generation by dielectric nanomaterials for quantum dots solar cells based on CdS-TiO₂ photoanode. *Sol Energy.* 2017; 158: 83-88.